Methane activation by nickel cluster cations, Ni_n^+ ($n=2-16$): Reaction mechanisms and thermochemistry of cluster-CH_x ($x=0-3$) complexes

Fuyi Liu, Xiao-Guang Zhang,[a] Rohana Liyanage,[b] and P. B. Armentrout
Department of Chemistry, University of Utah, Salt Lake City, Utah 84112

(Received 19 August 2004; accepted 16 September 2004)

The kinetic energy dependences of the reactions of Ni_n^+ ($n=2-16$) with CD_4 are studied in a guided ion beam tandem mass spectrometer over the energy range of 0–10 eV. The main products are hydride formation Ni_nD^+, dehydrogenation to form $Ni_nCD_2^+$, and double dehydrogenation yielding Ni_nC^+. These primary products decompose at higher energies to form Ni_nCD^+, $Ni_{n-1}D^+$, $Ni_{n-1}C^+$, $Ni_{n-1}CD^+$, and $Ni_{n-1}CD_2^+$. $Ni_nCD_2^+$ ($n=5-9$) and $Ni_{n-1}CD_2^+$ ($n\geqslant4$) are not observed. In general, the efficiencies of the single and double dehydrogenation processes increase with cluster size. All reactions exhibit thresholds, and cross sections for the various primary and secondary reactions are analyzed to yield reaction thresholds from which bond energies for nickel cluster cations to C, CD, CD_2, and CD_3 are determined. The relative magnitudes of these bond energies are consistent with simple bond order considerations. Bond energies for larger clusters rapidly reach relatively constant values, which are used to estimate the chemisorption energies of the C, CD, CD_2, and CD_3 molecular fragments to nickel surfaces. © *2004 American Institute of Physics.* [DOI: 10.1063/1.1814095]

I. INTRODUCTION

Transition metal clusters have been extensively investigated over the past two decades. Part of the interest in such species involves the transition from the atomic state to the bulk phase by observing the development of the physical and chemical properties with increasing cluster size. Clusters are often characterized by a high degree of coordinative unsaturation with a number of dangling bonds and, therefore, may be useful as models for catalysts.[1,2] In addition, clusters act as an ideal interface between experimental and theoretical studies. The size dependence of cluster reactivities is a fascinating and intriguing issue and has attracted much attention both theoretically and experimentally.[3–7] Our group has measured bond energies for transition metal cluster-ligand complexes[8–20] using guided ion beam tandem mass spectrometry. Surprisingly, these thermochemical values rapidly reach plateaus that are comparable to similar quantities for metal surfaces, when available. For example, in the $Fe_n^+ + D_2$ reaction system,[8] we found that Fe_n^+-D bond energies reach a relatively constant value of about 2.6 ± 0.1 eV for $n\geqslant10$, which is close to the bulk phase value of about 2.8 eV for hydrogen binding to bulk Fe(100), Fe(110), and Fe(111) surfaces.[21,22] Likewise, bond energies for Fe_n^+ to CD and CD_2 obtained from the $Fe_n^+ + CD_4$ reaction system reach plateaus of about 5.7 ± 0.4 and 4.2 ± 0.4 eV, respectively, for $n\geqslant10$.[15] These values are in reasonable agreement with values of 6.2 and 4.5 eV, respectively, estimated using a bond order conservation-Morse potential (BOC-MP) approach for binding to Fe/W(110) surfaces,[22] but no experimental data is available for such species. These data do suggest that the cluster-surface analogy provides relevant thermodynamic information for surface science and catalysis.

Surface catalytic reactions of CH_4 on nickel metal surfaces have been studied extensively because these reactions are involved in industrially important processes, such as steam reforming of methane and methanation of carbon monoxide.[23] The steam-reforming process, $CH_4+H_2O\rightarrow CO+3H_2$, transforms natural gas together with steam to synthesis gas (CO and H_2) over supported Ni catalysts, where the rate-limiting step is usually the dissociative chemisorption of methane on the nickel catalyst. This is often the first step in a chain of heterogeneous catalytic processes that generate more complicated chemical products from CO and H_2. Much fundamental experimental as well as theoretical work has been devoted to investigate the activation of methane and absorption of CH_x ($x=0-3$) species on nickel surfaces. From thermal experiments, activation energies for methane dissociation on Ni(111), (100), and (110) surfaces were found to lie in the range of 27–59 kJ/mol.[24–27] Nørskov and co-workers have suggested that these values are probably low because low pressures of methane do not allow efficient thermal equilibration between the gas phase and the single crystal surface.[28] Molecular beam experiments measured a state-resolved sticking coefficient curve from the lowest vibrational state of methane and give the estimated barrier height for dissociative chemisorption of methane as 70–90 kJ/mol.[29,30] Besides the translational energy in the beam, a key factor to determine the sticking coefficient is the internal energy of methane, which is believed to couple to a C–H bond stretch at the transition state. Such an interpretation was confirmed by calculations of the dynamics of CH_4 dissociation on a model potential energy surface.[31–33] The existence of adsorbed CH_3 and CH species on nickel sur-

[a]Present address: Department of Chemistry and Biochemistry, University of Texas at Austin, 1 University Station A5300, Austin, Texas 78712-0165.
[b]Present address: State Wide Mass Spectrometry Facility, University of Arkansas, Fayetteville, Arkansas 72701.

faces has been identified using high resolution electron energy loss spectrometry.[34,35] All CH_x $(x=0-3)$ fragments on a Ni(111) surface have been observed using secondary ion mass spectrometry.[36]

Theoretical studies of methane dissociation on nickel surfaces have been performed to predict the activation of the C–H bond and the relative stabilities of adsorbed CH_x species. Early work concentrated on the insertion of a single nickel atom into the C–H bond in methane[37] or followed a semiempirical approach to cluster models of adsorption.[38] Several *ab initio* studies at the configuration interaction level[39–41] addressed the chemisorption of CH_4 or CH_3 on a Ni(111) surface represented by cluster models. These studies reported a barrier of 71 kJ/mol for dissociative chemisorption of CH_4 to yield CH_3 and H on Ni(111) threefold hollow sites,[39] and of 63–71 kJ/mol on a Ni(100) surface modeled by a Ni_{13} cluster.[42] Density functional theory (DFT) has also been applied to study the dissociation of methane on various cluster models.[43,44] The calculated barrier heights are very sensitive to cluster size, ranging from 41 kJ/mol for single Ni atom insertion to 214 kJ/mol for Ni_7 and to 121 kJ/mol for Ni_{13}. Recent DFT calculations[45–50] investigated the adsorption of CH_4 and formation of CH_x $(x=0-3)$ on various nickel surfaces, providing barriers in the range of 100–109 kJ/mol for CH_4 activation and of 70–85 kJ/mol for further activation of the resultant CH_x $(x=1-3)$ species. The stability of CH_x fragments on different sites was also examined.

In the present study, we investigate the reactions of size-selected nickel cluster cations (2–16 atoms) with methane using guided ion beam tandem mass spectrometry. By measuring and analyzing the kinetic energy dependence of the reaction products from thermal energies to ≈10 eV, we are able to determine threshold energies for a number of processes and obtain bond energies for hydrocarbon molecular fragments, CH, CH_2, and CH_3, to size-specific nickel cluster cations. This investigation gives insight into C–H bond activation on nickel surfaces and provides quantitative thermodynamic information regarding the intermediates and products formed in these reactions. This thermodynamic information is compared to available experimental and theoretical estimates.

II. EXPERIMENT

The ion beam apparatus and experimental techniques used in this work have been described in detail elsewhere,[51] so only a brief description is given here. The formation of nickel cluster cations is achieved by laser vaporization/ionization and an ensuing expansion.[52] The output of a copper vapor laser (Oxford ACL 35, 511 and 578 nm, 3–4 mJ/pulse, operating at 7 kHz) is tightly focused onto a continuously translating and rotating nickel target rod inside an aluminum source block. The plasma is entrained in a continuous flow $[(5-6)\times 10^3$ SCCM (SCCM—cubic centimeter per minute at STP)] of He passing over the ablation surface. Frequent collisions and rapid mixing lead to the formation of thermalized clusters as they travel down a 2 mm diameter×63 mm long condensation tube. The gas mixture expands into a field-free region, is skimmed, and then passes through two differentially pumped regions. The expansion further cools the internal modes of the clusters so that these are assumed to be thermalized to near room temperature.[53–55]

The positively charged ions are extracted from the ion source, accelerated, focused, and injected into a 60° magnetic sector momentum analyzer. The mass selected ions are decelerated to a desired kinetic energy, and focused into a radio-frequency (rf) octopole ion guide[56] that extends through a reaction cell where the neutral gas CD_4 is introduced. The pressure of CD_4 neutral reactant gas (99.8% purity) in the reaction cell is kept relatively low (0.2–0.4 mTorr) to reduce the probability of multiple collisions with the ions. All reactions were conducted at two or more pressures of CD_4, which verified that all products observed are the result of single bimolecular encounters between the reactants. The octopole guide is biased with dc and rf voltages. The former allows us to accurately control the translational energy of the incoming ions, whereas the latter establishes a radial potential that efficiently traps the parent and product ions that travel through the octopole. The product and remaining reactant ions drift to the end of the octopole, where they are extracted and injected into a quadrupole mass filter for mass analysis. Finally, the ion intensities are measured with a Daly detector[57] coupled with standard pulse counting techniques. Reactant ion intensities used in these studies ranged from $(1-8)\times 10^5$ ions/s. Observed product-ion intensities are converted to absolute reaction cross sections on the basis of the 4π collection characteristics of the octopole, as discussed in detail elsewhere.[58] Absolute errors in the cross sections are on the order of ±30%.

Data collection for each reaction system was repeated several times to ensure reproducibility of results. Collision-induced dissociation (CID) experiments with Xe were performed on all the cluster ions to verify their identity and the absence of any excessive internal excitation. In all instances, CID thresholds are consistent with those previously reported.[55] The absolute zero in the kinetic energy of the ions and their energy distributions (the latter varying with cluster size from 0.7 to 2.0 eV) were measured using the octopole as a retarding energy analyzer. The error associated with the absolute energy scale is 0.05 eV in the lab frame. Kinetic energies in the laboratory frame are converted to center-of-mass (CM) energies using the stationary target approximation, $E(\mathrm{CM})=E(\mathrm{lab})\times m/(m+M)$, where m and M are the masses of the neutral and ionic reactants, respectively.[58] Unless stated, otherwise all energies quoted in the following correspond to the CM frame.

The products observed in this work include $Ni_nCD_x^+$ and Ni_nD^+ species where $x=0-3$. Accurate measurements of the intensities of these species is most conveniently accomplished by using deuterated methane to maximize the peak separation and by adjusting the resolution of the quadrupole mass filter to be as high as possible without reducing the product-ion intensities. In all cases, the cross sections reported below have been corrected for mass overlap with other species.

III. RESULTS

The reactions of nickel cluster cations, Ni_n^+ ($n = 2-16$), with CD_4 were studied varying the relative kinetic energy over a range of thermal to 10 eV in the center-of-mass frame. Deuterated methane was used to enhance the mass separation between products. To help organize the results of the myriad reactions observed, we first note which processes are possible and observed in at least one of the cluster systems. These can be classified into reactions in which no loss of nickel atoms occurs, processes (1)–(5):

$$Ni_n^+ + CD_4 \rightarrow Ni_nD^+ + CD_3 \quad (1)$$

$$\rightarrow Ni_nC^+ + 2D_2 \quad (2)$$

$$\rightarrow Ni_nCD^+ + D + D_2 \quad (3)$$

$$\rightarrow Ni_nCD_2^+ + D_2 \quad (4)$$

$$\rightarrow Ni_nCD_3^+ + D. \quad (5)$$

At higher energies, products having fewer nickel atoms are formed in dissociations of the products formed in reactions (1)–(5). Reactions (6)–(10) comprise the latter types of processes observed:

$$Ni_n^+ + CD_4 \rightarrow Ni_{n-1}D^+ + Ni + CD_3 \quad (6a)$$

$$\rightarrow Ni_{n-1}D^+ + NiCD_3 \quad (6b)$$

$$\rightarrow Ni_{n-1}C^+ + Ni + 2D_2 \quad (7)$$

$$\rightarrow Ni_{n-1}CD^+ + NiD + D_2 \quad (8)$$

$$\rightarrow Ni_{n-1}CD_2^+ + Ni + D_2 \quad (9)$$

$$\rightarrow Ni_{n-1}CD_3^+ + NiD. \quad (10)$$

The only other products observed are formed in the simple collision-induced dissociation reaction (11):

$$Ni_n^+ + CD_4 \rightarrow Ni_{n-1}^+ + Ni + CD_4. \quad (11)$$

In most cases, the identity of the concomitant neutral products is obvious but in reactions (6), (8), and (10), two pathways are possible and identification of the observed pathways relies on thermodynamic arguments, as discussed below. For reactions (8) and (10), these thermodynamic arguments are used to discount formation of the alternate neutral products, Ni+D rather than NiD. As noted above, the pressure dependences of the cross sections demonstrate that all reactions observed result from a single collision between nickel cluster cations and methane.

A. $Ni^+ + CD_4$

Previous experiments[59] have shown that only endothermic processes, reactions (1), (4), and (5), occur in the interactions of atomic nickel ions with methane. The product ion, NiH^+, dominates the product spectrum at all energies examined. Smaller amounts of $NiCH_2^+$ and $NiCH_3^+$ are also observed and account for about 12% of the total product distribution. A more detailed study of this reaction system using the present experimental apparatus also finds the minor products, $NiCH^+$ and NiC^+, at higher energies.[60] This study also measures a barrier in excess of the endothermicity for dehydrogenation of methane by Ni^+ as 0.58 ± 0.10 eV. This value is in good agreement with that calculated by theory, which attributes the barrier to a four-centered transition state in the H_2 elimination step of the reaction.[60]

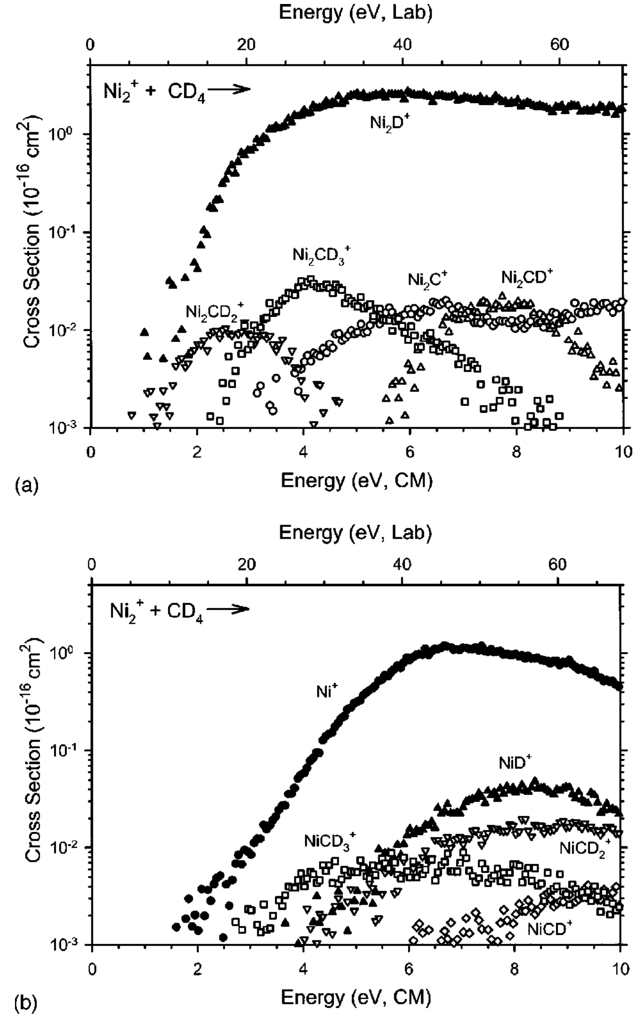

FIG. 1. Product cross sections for the reaction of Ni_2^+ with CD_4 as a function of collision energy in the center of mass (lower x axis) and laboratory axis (upper x axis). Parts (a) and (b) show Ni_2L^+ and NiL^+ cross sections, respectively.

B. $Ni_2^+ + CD_4$

Addition of a second nickel atom to the reactant cluster ion greatly increases the complexity of the reaction system. Figure 1 shows results for reaction of the nickel dimer cation with methane. A number of different products are formed in reactions (1)–(6) and (8)–(11), which are all endothermic. The dominant process at all energies is formation of Ni_2D^+ in reaction (1). At higher energies, Ni_2D^+ can lose a nickel atom to form NiD^+ in reaction (6a). The CID product formed in reaction (11) is also important, with a cross section magnitude comparable to that of Ni_2D^+ at higher energies. This is reasonable given that the nickel dimer cation has the weakest bond energy of all nickel cluster cations.[55]

The lowest energy process in reaction of Ni_2^+ with methane is the formation of $Ni_2CD_2^+$ in reaction (4), with an apparent threshold about 1 eV lower than dehydrogenation by Ni^+. At higher energies, $Ni_2CD_2^+$ can dissociate by nickel atom loss to form $NiCD_2^+$ in reaction (9), by further dehydrogenation to form Ni_2C^+ in reaction (2), and by deuterium atom loss to yield Ni_2CD^+ in reaction (3). The latter two channels show some competition with one another as the cross section magnitude for Ni_2C^+ decreases when the Ni_2CD^+ product appears and Ni_2C^+ increases again at about 8 eV when the Ni_2CD^+ product decreases. The $Ni_2CD_3^+$ product reaches a maximum near 4 eV, suggesting that it decomposes primarily by CD_3 loss, which can begin at $4.58\,\mathrm{eV}=D(\mathrm{D{-}CD_3})$. Ni_2CD^+ can also decompose further by nickel atom loss to form $NiCD^+$, a product that may also be formed by D atom loss from $NiCD_2^+$, by D_2 loss from $NiCD_3^+$, or by NiD loss from $Ni_2CD_2^+$. As discussed below, concomitant formation of NiD is suggested by thermodynamic arguments for formation of $NiCD^+$ at the threshold, as well as for the $NiCD_3^+$ product, reaction (10). It seems likely that the failure to see NiC^+, reaction (7), is simply because its intensity is too small.

C. Ni_3^+ and $Ni_4^+ + CD_4$

Cross sections for the nickel trimer cation reaction with methane are shown in Fig. 2, where reactions (1)–(4), (6)–(11) are all observed. The results are similar to those of the dimer, however, dehydrogenation, reaction (4), is much more prominent and the $Ni_3CD_3^+$ product of reaction (5) is absent in this system. Dehydrogenation is the lowest energy reaction of the trimer, with an apparent threshold about 1 eV lower than deuteride formation in reaction (1). The $Ni_3CD_2^+$ cross section reaches a maximum at the energy where this product can further dehydrogenate to form Ni_3C^+. This product can also decompose by losing a D atom to form Ni_3CD^+ and a nickel atom to form $Ni_2CD_2^+$. Dehydrogenation is the dominant dissociation channel. The magnitude of these three decomposition channels nearly account for the decline in the $Ni_3CD_2^+$ cross section, but there is break in the sum of these four cross sections near 2.5 eV. The only channel large enough to account for this behavior is the Ni_3D^+ channel. This indicates that the primary products, $Ni_3CD_2^+$ and Ni_3D^+, must compete with each other, which suggests that they share a common precursor, as discussed further below.

Ni_3D^+ and Ni_2^+ are the main products at higher energies. Ni_2D^+, formed by nickel atom loss from Ni_3D^+ in reaction (6a), is also quite important in this system, a consequence of Ni_2^+-D being a relatively strong bond.[17] As for the dimer, the primary $Ni_3CD_x^+$ products decompose to yield $Ni_2CD_x^+$ products in reactions (7)–(9). Possible pathways for Ni_2CD^+ and Ni_2C^+ production involve loss of a nickel atom from the Ni_3CD^+ and Ni_3C^+ products, respectively, loss of D and D_2 from $Ni_2CD_2^+$, respectively, or the former product can be formed by loss of NiD from $Ni_3CD_2^+$ or D_2 loss from $Ni_2CD_3^+$. On the basis of the measured thresholds and shapes of the cross sections, Ni_2CD^+ appears to be formed primarily by NiD loss from $Ni_3CD_2^+$, and Ni_2C^+ is produced by a nickel atom loss from Ni_3C^+. Formation of $Ni_2CD_3^+$ is observed with a threshold that corresponds to production of a NiD neutral in reaction (10), see below. This

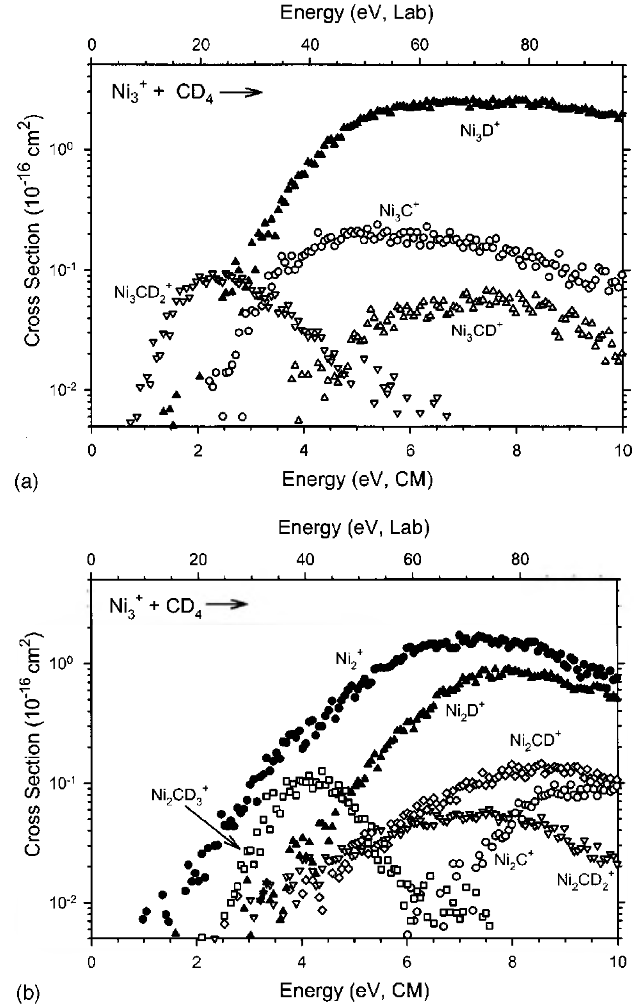

FIG. 2. Product cross sections for the reaction of Ni_3^+ with CD_4 as a function of collision energy in the center of mass (lower x axis) and laboratory axis (upper x axis). Parts (a) and (b) show Ni_3L^+ and Ni_2L^+ cross sections, respectively.

product is unlikely to be formed by Ni loss from $Ni_3CD_3^+$, as no $Ni_3CD_3^+$ is observed.

Reaction cross sections for the nickel tetramer cation shown in Fig. 3 are similar to those for reaction of the nickel trimer cation with methane in many respects. Reactions (1)–(4), (6)–(8) and (11) are all observed, but unlike the smaller clusters, no methylated cluster products or $Ni_3CD_2^+$ products are observed. A striking feature of these results is the virtual absence of the dehydrogenation product, $Ni_4CD_2^+$. However, this species must be formed transiently as double dehydrogenation, reaction (2), is efficient and reaction (3) almost certainly occurs via this primary product as well. Further, Ni_3CD^+ is also observed and is likely to be formed by NiD loss from $Ni_4CD_2^+$, according to the apparent threshold. As for the trimer system, the Ni_4C^+ product declines because of competition with Ni_4D^+ formation, as no other product has a cross section with sufficient magnitude to account for the decline.

D. Ni_n^+ ($n=5-9$) $+CD_4$

Figure 4 shows the cross sections for reaction of nickel heptamer cation with methane, which are representative of

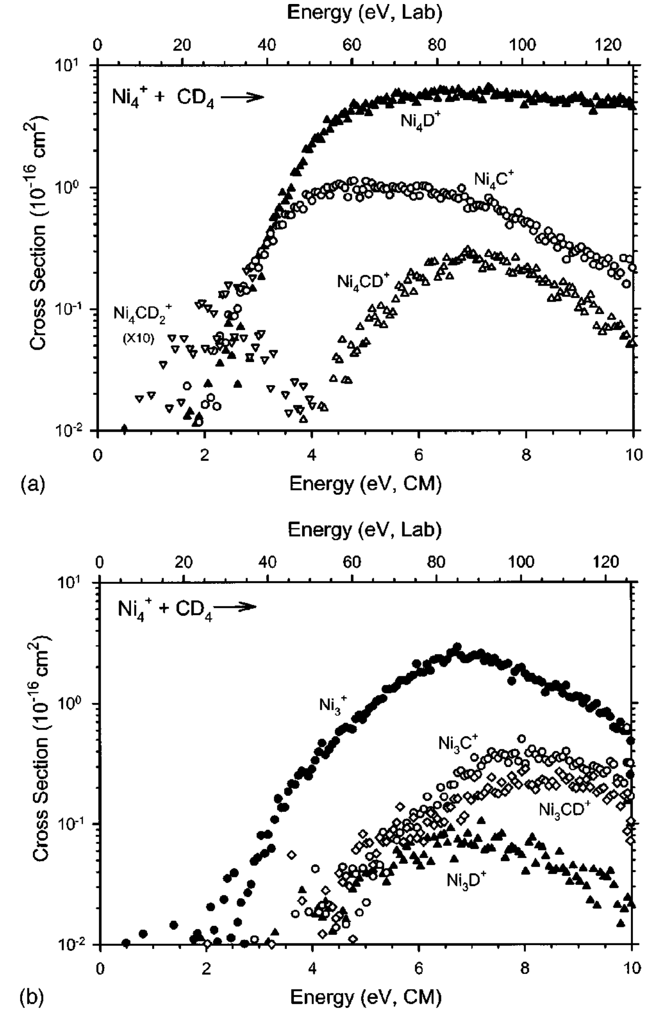

FIG. 3. Product cross sections for the reaction of Ni_4^+ with CD_4 as a function of collision energy in the center of mass (lower x axis) and laboratory axis (upper x axis). Parts (a) and (b) show Ni_4L^+ and Ni_3L^+ cross sections, respectively.

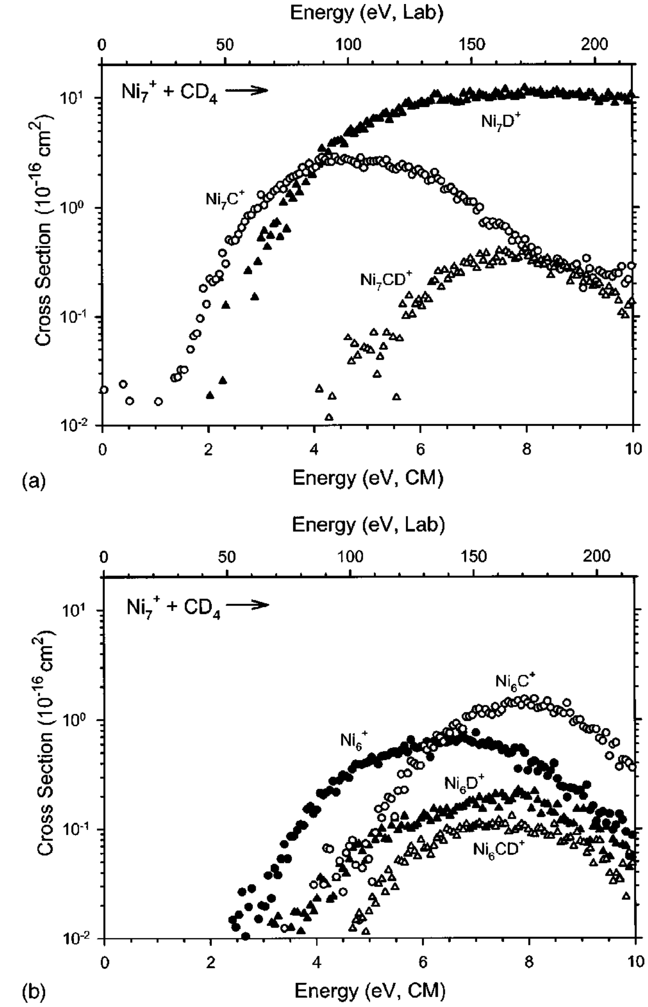

FIG. 4. Product cross sections for the reaction of Ni_7^+ with CD_4 as a function of collision energy in the center of mass (lower x axis) and laboratory axis (upper x axis). Parts (a) and (b) show Ni_7L^+ and Ni_6L^+ cross sections, respectively.

the $n=5-9$ clusters (see Figs. 1*S*–4*S*).[75] Reactions (1)–(3), (6)–(8), and (11) are observed. In contrast to smaller clusters, the dehydrogenation products, $Ni_nCD_2^+$ and $Ni_{n-1}CD_2^+$, are absent for the $n=5-9$ clusters. However, $Ni_nCD_2^+$ must be formed transiently as the double dehydrogenations, forming Ni_nC^+, are quite facile, and Ni_nCD^+ and $Ni_{n-1}CD^+$ almost certainly are formed via this primary product as well. The absence of $Ni_{n-1}CD_2^+$ means that $Ni_nCD_2^+$ prefers to decompose by double dehydrogenation, and even D atom loss is preferred to a Ni atom loss pathway. The magnitudes of the Ni_nC^+ $(n=5-9)$ cross sections (2–3 Å^2 maximum) are about two to three times larger than for the tetramer, and the apparent thresholds for these products are shifted to lower energies. Similar to the reactions of smaller clusters, the Ni_nC^+ cross sections decline largely because of competition with Ni_nD^+ formation. The Ni_nD^+ cross sections are about twice as large as for the tetramer.

E. Ni_n^+ $(n=10-16)+CD_4$

Figure 5 shows results for reactions of the nickel dodecamer cation with methane, which are representative of larger clusters $(n=10-16)$ (see Figs. 5*S*–10*S*).[75] Reactions (1)–(4), (6)–(8), and (11) are observed in all cases, although the quality of the data for reactions (6)–(8) was poor for the largest clusters. In contrast to the Ni_n^+ $(n=5-9)$ clusters, the dehydrogenation product, $Ni_nCD_2^+$, is again observed with a gradual increase in the maximum magnitude as the cluster size increases, from 0.1 Å^2 for $n=10$ to about 3.5 Å^2 for $n=15$ and 16. The double dehydrogenation reactions to form Ni_nC^+ are much more facile in these systems, such that Ni_nC^+ are the dominant products over a 2–4 eV range. $Ni_{n-1}CD_2^+$ products are not observed for these larger clusters. Formations of the secondary $Ni_{n-1}D^+$, $Ni_{n-1}C^+$, and $Ni_{n-1}CD^+$ products are similar to those for the smaller clusters.

IV. THRESHOLD ANALYSIS AND THERMOCHEMISTRY

A. Data analysis

Previous theoretical[61] and experimental[62,63] work has shown that endothermic cross sections in the threshold region can be modeled using Eq. (12),

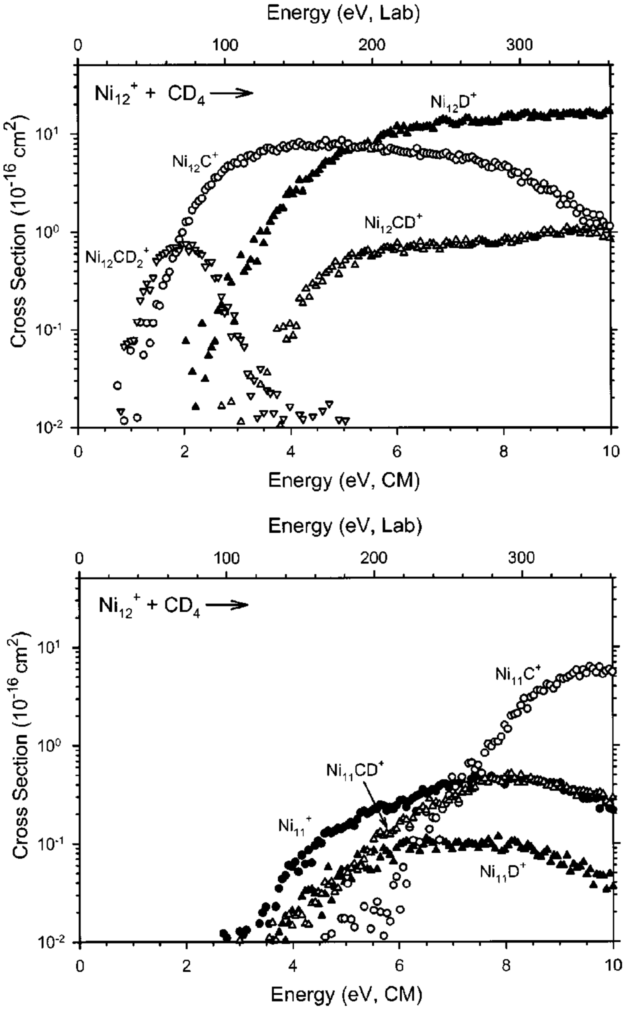

FIG. 5. Product cross sections for the reaction of Ni_{12}^+ with CD_4 as a function of collision energy in the center of mass (lower x axis) and laboratory axis (upper x axis). Parts (a) and (b) show $Ni_{12}L^+$ and $Ni_{11}L^+$ cross sections, respectively.

$$\sigma(E)=\sigma_0\sum g_i(E+E_i-E_0)^N/E, \tag{12}$$

where σ_0 is an energy independent scaling parameter, N is an adjustable parameter that describes the energy dependence,[64] E is the relative kinetic energy, and E_0 is the threshold for reaction at 0 K. The summation is over the rovibrational states of the clusters having energies E_i and relative populations g_i, where $\Sigma g_i=1$, which are calculated using a Maxwell-Boltzmann distribution at 300 K. Vibrational frequencies for the bare metal clusters are obtained by using a elastic cluster model suggested by Shvartsburg *et al.*[65] A characteristic of this approach is the formal assignment of the vibrational models to one longitudinal and two transverse branches. The parameters used in this study are the Debye frequency for bulk nickel, $v_D(\infty)=268\ \mathrm{cm}^{-1}$,[66] the bulk maximum longitudinal frequency, $v_{L,\max}=296\ \mathrm{cm}^{-1}$,[66] and the ratio of the longitudinal to the transverse phonon velocity, $c_L/c_T=1.79$.[67] The vibrational frequencies of CD_4 used in this work are taken from the literature.[68] This model cross section, Eq. (12), is also convoluted with the kinetic energy distributions of the ion and neutral reactants before comparison with the experimental data.[58]

For metal clusters, it has been shown that lifetime effects become increasingly important as the size of the cluster increases[55] and have to be explicitly treated for the extraction of accurate thermochemical data from threshold experiments.[3,63,69,70] This is because metal clusters have many low frequency vibrational modes such that energy redistribution in the transient intermediate is very effective. Hence, the lifetimes of some reaction intermediates can exceed the experimental time window ($\approx 10^{-4}$ s in our apparatus) available for reaction. This results in a kinetic shift of the experimental thresholds to energies higher than the thermochemical endothermicity. Thus, an important component of the modeling of these reactions is to include the reaction kinetics, as estimated using statistical Rice–Ramsperger–Kassel–Marcus (RRKM) theory.[71–73] This is achieved using an extension of Eq. (12), detailed elsewhere,[74] and requires molecular constants for the energized molecule (EM) and transition state (TS) leading to the product of interest. Three different transition state models are employed: (a) a loose variational transition state (LTS); (b) a tight fixed transition state (TTS); and (c) a "standard" tight, fixed transition state (STS). A more complete description of these TS models, along with detailed explanations for their choices and the molecular constants used for the EMs and TSs for all reactions are provided in the supplementary material.[75] For all secondary reactions (where at least two neutral products are formed), product cross sections were analyzed by removing the energy needed to generate the precursor (EM) for the process under consideration. For instance, during the analysis of Ni_nC^+ product cross section, the threshold energy measured for the $Ni_nCD_2^+$ precursor is removed from the total energy as that energy is not available for D_2 loss from $Ni_nCD_2^+$.

B. Primary and secondary reactions

A fortunate aspect of cluster studies is the observation of identical product ions formed in both primary and secondary reactions. Thus, a species like Ni_nL^+ is formed as a primary product of Ni_n^+ in reaction (13), and a secondary product of Ni_{n+1}^+ in reactions (14) or (15),

$$Ni_n^+ + CD_4 \rightarrow Ni_nL^+ + (CD_4-L), \tag{13}$$

$$Ni_{n+1}^+ + CD_4 \rightarrow Ni_nL^+ + Ni + (CD_4-L), \tag{14}$$

$$Ni_{n+1}^+ + CD_4 \rightarrow Ni_nL^+ + Ni(CD_4-L), \tag{15}$$

where (CD_4-L) is the fragment remaining after removing L from CD_4. Hence, we generally have two independent means of determining the thermochemistry of each of the Ni_nL^+ products. It is conceivable that thresholds obtained for the secondary reactions (14) could be higher than thermodynamic values if the total energy available in reaction (14) is not efficiently retained by $Ni_{n+1}L^+$ precursors. However, if we assume the energy is divided among the primary products statistically, we can expect that the $Ni_{n+1}L^+$ product will retain much more energy than the CD_4-L product,

TABLE I. Ni_n^+–D bond energies (eV) obtained from the literature and analyses of reactions (1) and (6).

	Ni_n^+–D[a]	Ni_n^+–D (1)[b]	Ni_n^+–D (6a)[c]	Ni_n^+–D (6b)[c]
1	1.72±0.08[d]		1.68±0.16	
2	3.04±0.10	2.88±0.09	2.87±0.16	
3	2.00±0.10	1.71±0.14	2.13±0.25	
4	1.94±0.16	1.78±0.11	1.93±0.29	
5	2.09±0.15	2.12±0.12	2.13±0.31	
6	2.26±0.19	2.20±0.12	4.02±0.33	2.15±0.38
7	2.21±0.28	2.14±0.13	4.00±0.36	2.01±0.38
8	2.10±0.41	2.07±0.09		2.28±0.41
9	2.24±0.34	2.26±0.12		2.08±0.43
10	2.42±0.33	2.44±0.15		2.70±0.42
11	2.63±0.38	2.53±0.11		2.77±0.45
12	2.48±0.35	2.51±0.13		2.59±0.45
13	2.60±0.34	2.44±0.15		
14	2.64±0.34	2.52±0.14		
15	2.55±0.38	2.56±0.15		
16	2.67±0.37	2.57±0.14		

[a]From reactions of $Ni_2^+ + D_2$, Ref. 17.
[b]Values obtained from analyses of reactions (1) assuming LTS and explicit competition with reactions (4).
[c]Average bond energies obtained from analyses of $Ni_{n-1}D^+$ cross sections assigned to reactions (6a) or (6b) assuming LTS and STS models.
[d]Reference 92.

which has many fewer degrees of freedom. Similar considerations hold for alternate mechanistic pathways for the secondary reactions. Clearly, this assumption could degrade for the smallest clusters and we explicitly consider this question below. Similar considerations were also explored in our recent studies on $Fe_n^+ + CD_4$ and ND_3, and Fe_n^+ and $Fe_nS^+ + COS$ and CS_2.[15,18,20] The comparisons of bond energies obtained from the primary and secondary processes in these systems showed the basic validity of these assumptions.

Optimized modeling parameters of Eq. (12) for the analyses of all reactions are given in the supplementary material.[75] Bond energies of interest can be obtained from the thresholds for reactions (13)–(15) utilizing Eqs. (16)–(18),

$$D(Ni_n^+-L) = D(CD_4-L) - E_0(13), \tag{16}$$

$$D(Ni_n^+-L) = D(CD_4-L) + D(Ni_n^+-Ni) - E_0(14), \tag{17}$$

$$D(Ni_n^+-L) = D(CD_4-L) + D(Ni_n^+-Ni) - E_0(15) - D[Ni-(CD_4-L)], \tag{18}$$

where $D(CD_4-L)$ is the energy required to remove L from CD_4. In Eqs. (17) and (18), the dissociation energies for the bare Ni_n^+ clusters are taken from previous studies in our laboratory.[55,76] In the present work, neutral $Ni(CD_4-L)$ species observed include only NiD and $NiCD_3$, which have bond energies of 2.48±0.08 and 2.20±0.08 eV, respectively.[77]

C. Thermochemical results

1. Ni_n^+–D

Bond energies for Ni_nD^+ have previously been measured by threshold analyses of the endothermic reactions of Ni_n^+ clusters with D_2,[17] and are listed in Table I. In the present study, this thermochemistry can be obtained from analyses of the cross sections for reactions (1), (6a), and (6b). Needed thermodynamic information includes $D(CD_3-D) = 4.58 \pm 0.01$ eV (Ref. 78) and $D(Ni-CD_3) = 2.20 \pm 0.08$ eV.[77] As detailed in the supplementary material,[75] reactions (1) were analyzed using a LTS coupled with explicit consideration of the competition[79] with the low energy dehydrogenation channel, reaction (4), assumed to have a TTS. Bond energies obtained from these analyses are listed in Table I and shown as open circles in Fig. 11S.[75] These values are in good agreement with the previous data,[17] with a mean absolute deviation (MAD) of 0.09±0.08 eV for $n = 2-16$. It is worth stressing that the competition threshold analysis has no additional optimizing parameters (other than the threshold energies for each channel) to adjust compared to the normal threshold analysis (including lifetime effects).[79] The competition between channels is determined by the ratio of the unimolecular rate constants for each process, as calculated using RRKM theory. Thresholds for both reactions (1) and (4) are simultaneously obtained in this procedure.

Ni_n^+–D bond energies obtained from analyses of the secondary reactions (6a) are listed in Table I (see also Fig. 11S). As detailed in the supplementary material,[75] the data for reactions (6a) were analyzed assuming both a LTS and a STS. The average bond energies obtained using these two models are in good agreement with the previously published values[17] up to $n = 5$ (MAD=0.08±0.07 eV for $n = 1-5$). Hence, our assumption that energy is efficiently retained by the primary product (Ni_nD^+) appears to be reasonable, even for these smaller clusters. For clusters larger than $n = 6$, modeling of the $Ni_{n-1}D^+$ cross sections over extended energy regions using Eq. (12) requires large values of the parameter N and leads to thresholds corresponding to bond energies that are too large given the assumption that reaction (6a) is operative. For example, the bond energies derived for $n = 6$ and 7 exceed the literature values by 1.76±0.38 and 1.79±0.46 eV, respectively. These differences are within experimental error of the Ni–CD_3 bond energy of 2.20±0.08 eV;[77] hence, contributions to these cross sections from reactions (6b) are indicated. Therefore, we analyze the cross sections at the lowest energies for reaction of clusters $n = 7-13$ and assign these thresholds to reaction (6b), Tables S2–S16. This leads to the bond energies for $n = 6-12$ given in Table I and shown in Fig. 11S.[75] These values are in good agreement with the previous data,[17] MAD=0.17±0.06 eV.

2. Ni_n^+–CD_3

Nickel cluster methyl cations are observed only in the reactions of the dimer and trimer cations. For dimer reactions, the thresholds for $Ni_2CD_3^+$ and $NiCD_3^+$ are 2.45±0.09 and 2.44±0.15 eV, respectively. The bond energy $D_0(Ni_2^+-CD_3)$ of 2.13±0.09 eV can be obtained according to Eq. (16). If we assume that the secondary methyl product is formed along with NiD in reaction (10), Eq. (18) can be used to convert the latter threshold to a Ni^+-CD_3 bond energy of 1.77±0.18 eV. This value for $NiCD_3^+$ agrees with a bond energy previously determined for $NiCH_3^+$, 1.94±0.06 eV.[76] The alternate assumption of concomitant formation of

TABLE II. Ni_n^+-C bond energies (eV) obtained from analyses of reactions (2) and (7).

n	Ni_n^+-C (2,TTS)	Ni_n^+-C (7)[a]
1	2.6[b]	
2	4.74±0.12	4.45±0.17
3	5.72±0.09	5.46±0.27
4	5.85±0.11	5.85±0.27
5	6.45±0.12	6.55±0.30
6	6.31±0.10	6.49±0.35
7	6.36±0.11	6.14±0.38
8	6.27±0.14	6.04±0.41
9	6.20±0.13	6.24±0.43
10	6.46±0.17	6.12±0.48
11	6.44±0.17	6.34±0.48
12	6.41±0.16	6.41±0.51
13	6.46±0.19	6.13±0.50
14	6.66±0.18	6.49±0.52
15	6.67±0.18	
16	6.62±0.20	

[a]Average bond energies obtained from LTS and STS models.
[b]Reference 60.

TABLE III. Ni_n^+-CD bond energies (eV) obtained from analyses of reactions (3) and (8).

n	Ni_n^+-CD (3,LTS)	Ni_n^+-CD (8)[a]
1	3.12±0.12[b]	3.41±0.21
2	4.83±0.12	4.83±0.19
3	5.26±0.14	5.07±0.32
4	5.10±0.12	5.12±0.30
5	5.14±0.15	5.24±0.35
6	5.07±0.17	5.26±0.35
7	4.91±0.20	5.10±0.38
8	5.27±0.21	5.57±0.40
9	5.33±0.20	5.54±0.45
10	5.71±0.21	6.01±0.49
11	5.70±0.21	5.85±0.48
12	5.86±0.19	6.04±0.50
13	5.95±0.27	5.72±0.47
14	6.04±0.25	5.97±0.50
15	6.01±0.21	
16	6.09±0.21	

[a]Average bond energies obtained from LTS and STS models.
[b]Reference 60.

Ni+D yields a bond energy of 4.25±0.17 eV for Ni^+-CD_3, much too large to be reasonable. Clearly, $NiCD_3^+$ is formed in process (10) along with NiD as a neutral product for reaction of the dimer. For the trimer, only a secondary methyl product is observed in reaction (10). The bond energy $D_0(Ni_2^+-CD_3)=2.00\pm0.18$ eV can be obtained from the threshold (2.54±0.11 eV) using Eq. (18). This value is in reasonable agreement with that obtained from the dimer reaction within experimental uncertainty. Thus, loss of neutral NiD to form this methyl product is also certain for the trimer reaction. We take the weighted average value of 2.10±0.16 eV as our best determination of the $Ni_2^+-CD_3$ bond energy. Larger clusters do not produce $Ni_nCD_3^+$ or $Ni_{n-1}CD_3^+$ with any efficiency, apparently because the transient $Ni_nCD_4^+$ intermediates have more facile decomposition pathways than loss of D or NiD, respectively.

3. Ni_n^+-C and Ni_n^+-CD

Bond energies for Ni_n^+-C can be obtained from analyses of reactions (2) and (7). Here, the required thermochemistry is $D(CD_4-L)=D(CD_2-D_2)+D(C-D_2)=8.20\pm0.04$ eV.[78] For reactions (2), the precursors are the primary $Ni_nCD_2^+$ products, whereas for reactions (7), they are the Ni_nC^+ products. The appropriate TSs are outlined in the supplementary material. The average bond energies obtained from reactions (7) using the average of LTS and STS models do not agree well with results obtained from analyses of reactions (2) using a LTS model, but do agree well with results for reactions (2) if a TTS model is used (MAD=0.17±0.12 eV). Hence, we conclude that reactions (2) proceed via a TTS. These bond energies are listed in Table II and shown in Fig. 12S.[75] Thresholds from the primary reactions (2) are more precise and therefore taken to be our best determination of bond energies for several reasons:

(a) The mass overlap adjustments for the Ni_nC^+ cross sections are less ambiguous compared to those for the $Ni_{n-1}C^+$ cross sections.

(b) Thresholds for reactions (7) occur at high energies, such that there are fewer data points for modeling given our energy range of 10 eV.

(c) Thresholds for reactions (7) could be shifted to higher energies by competition with the more efficient low energy processes or shifted as a consequence of the multiple neutral products carrying away excess energy.

Bond energies for Ni_n^+-CD can be obtained from analyses of reactions (3) and (8). The required thermochemistry is $D(CD_4-L)=D(CD_2-D_2)+D(CD-D)=9.25\pm0.04$ eV (Ref. 78) and $D(Ni-D)=2.48\pm0.08$ eV.[77] For reactions (3) and (8), the precursors are the primary $Ni_nCD_2^+$ products, as discussed above. Therefore, cross sections are analyzed for thresholds using LTS models associated with D atom loss for reactions (3) and NiD loss for reactions (8). The results are given in Table III and also shown in Fig. 13S of the supplementary material.[75] Bond energies obtained from analyses of reactions (8) are in good agreement with bond energies obtained from reactions (3) (MAD=0.17±0.09 eV), and lie within the experimental errors. Note that if Ni_{n-1}^+-CD products were formed with D_2+Ni+D instead of with D_2+NiD, the agreement with the bond energies from reaction (3) would not be obtained. Of these two sets of bond energies, those obtained from analyses of the primary reactions (3) are the most reliable and precise for the same reasons as those listed above for the Ni_n^+-C bond energies.

4. $Ni_n^+-CD_2$

Bond energies for $Ni_n^+-CD_2$ can be obtained from analyses of the thresholds for reactions (4) and (9) using Eqs. (16) and (17), respectively, and $D(CD_2-D_2)=4.82\pm0.03$ eV.[78] As discussed above, the data for reactions (4) were analyzed assuming both a LTS and a TTS. Competition with reaction (1) is also explicitly considered but this does not alter the thresholds obtained for reaction (4). The resultant bond energies are listed in Table IV and show that values derived assuming a LTS average 0.33±0.03 eV lower than those for a TTS for $n=10-16$. Secondary reactions (9) cor-

TABLE IV. $Ni_n^+-CD_2$ bond energies (eV) obtained from analyses of reactions (4) and (9).

n	$Ni_n^+-CD_2$ (4,LTS)	$Ni_n^+-CD_2$ (4,TTS)	$Ni_n^+-CD_2$ (9)[a]
1		3.17±0.04[b]	3.16±0.16
2	3.77±0.09	3.79±0.09	4.40±0.18
3	3.84±0.08	3.87±0.08	
4	~3.3[c]	~3.6[c]	
10	~3.5[c]	~3.8[c]	
11	3.55±0.08	3.86±0.08	
12	3.59±0.09	3.92±0.09	
13	3.60±0.09	3.93±0.10	
14	3.66±0.09	4.00±0.11	
15	3.69±0.10	4.04±0.10	
16	3.63±0.10	4.01±0.12	

[a]Average bond energy obtained from LTS and STS models.
[b]References 76 and 80.
[c]Because of the small size of these cross sections, only rough estimates of the threshold could be obtained.

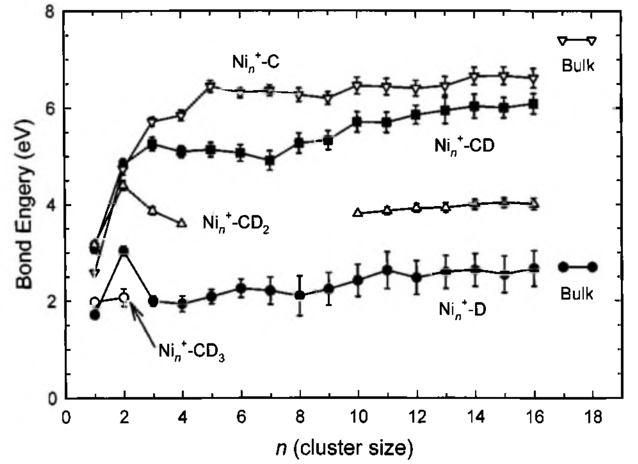

FIG. 6. Comparison of bond energies for Ni_n^+-D (solid circles, taken from Ref. 17), $Ni_n^+-CD_3$ (open circles, Ref. 76 and this work), $Ni_n^+-CD_2$ (open triangles, Ref. 76 and this work, Table IV, see text), Ni_n^+-CD (solid squares, this work, Table III), and Ni_n^+-C (open inverted triangles, this work, Table II). Bulk phase values for nickel surfaces binding D (Refs. 17 and 86) and C (Ref. 87, see text) are also shown.

responding to loss of a Ni atom from the $Ni_nCD_2^+$ primary products are only observed for reactions of the dimer and trimer cations. Here the transition states may be treated with LTS or STS models.

For reaction of Ni_2^+ to form $NiCD_2^+$ in process (9), the thresholds obtained using LTS and STS models correspond to Ni^+-CD_2 bond energies of 3.06±0.16 and 3.26±0.15 eV, for an average value of 3.16±0.16 eV, Table IV. All these values are in good agreement with the literature bond energy, 3.17±0.04 eV.[76,80] These bond energies lie above that derived from the threshold measurement of reaction (4) with $n=1$, 2.64±0.09 eV, Table IV, but this value is low because there is a barrier of 0.58±0.10 eV to this reaction, as demonstrated by examining the reverse process, $NiCH_2^+ + D_2 \rightarrow Ni^+ + CH_2D_2$.[60] This barrier is attributed to a four-center transition state in the exit channel, as verified by theoretical calculations.[60]

For reaction of Ni_3^+ to form $Ni_2CD_2^+$, the thresholds obtained from analysis of reaction (9) using a LTS corresponds to bond energy of 4.27±0.18 eV, well above the value derived from reaction (4), 3.79±0.09 eV, Table IV. The result for reaction (9) is not particularly sensitive to the type of transition state as the bond energy obtained using a STS is 4.53±0.17 eV. In analogy with the dimer reaction, the discrepancy between the results for the primary and secondary reactions is sensibly attributed to a barrier along the reaction path for dehydrogenation in reaction (4). This indicates that the use of the TTS model for reaction (4) is appropriate. For reaction of the trimer cation, this barrier is measured to be about 0.61±0.20 eV, comparable to the value for the monomer.

Unfortunately, the secondary reactions (9) are observed only in dimer and trimer reactions and reactions (4) are not observed for clusters from $n=5$ to 9 in our experiments. In the dehydrogenation reactions of larger iron cluster cations with methane,[15] primary and secondary paths were observed for all cluster sizes. This allowed us to ascertain that the primary dehydrogenation reactions exhibited barriers, assigned to the entrance channel, for Fe_n^+ ($n=5-15$). The barrier height averaged 0.7±0.3 eV. In analogy with these results, the primary dehydrogenation reactions for larger nickel clusters seem likely to have barriers in the entrance channel as well. Thus, bond energies $D(Ni_n^+-CD_2)$ ($n=3,4,10-16$) obtained here for reactions (4) using a TTS model are conservatively thought to be lower limits to the true thermochemistry.

V. DISCUSSION

A. Bond energies

Our recommended bond energies between nickel cluster cations and the D and CD_x ($x=0-3$) ligands are shown in Fig. 6. The Ni_n^+-D values are taken from our previous work on reactions of $Ni_n^+ + D_2$.[17] Results from the present study substantiate these values but analyses of the D_2 reaction cross sections are easier than for the CD_4 reaction system because there is no competition with other products in the D_2 system. The Ni_n^+-C values are those derived from analyses of reactions (2) with a TTS in all cases, Table II; whereas those for Ni_n^+-CD are LTS results for reactions (3), Table III. As noted above, the latter two sets of values are substantiated reasonably well by results for the secondary reactions (7) and (8), respectively. The $Ni_n^+-CD_2$ values, Table IV, are obtained as the lower limits from reactions (4) using a TTS model, except for the $NiCD_2^+$ and $Ni_2CD_2^+$ values. The former is taken from the literature,[76,80] and the latter is obtained from reaction (9) using the average thresholds obtained from LTS and STS models.

In general, the trends in these cluster-ligand bond energies can be understood by considering the maximum number of bonds that the ligands can make with the cluster. $D(^2S)$ and CD_3 $(^2A_1)$ can make only a single covalent bond with the cluster, whereas CD_2 $(^3B_2)$ can make two covalent bonds. CD can make three covalent bonds, but this requires promotion to the $\tilde{a}\,^4\Sigma^-$ state, which is 0.72 eV above the $X\,^2\Pi_r$ ground state.[81] The carbon atom has a ground state electronic configuration of $(2s)^2(2p)^2$ such that it can form two covalent bonds and accept electron density into the empty $2p$ orbital to form a third, dative bond. It can be seen that the Ni^+-D and Ni^+-CD_3 bond energies are comparable, whereas the Ni_2^+-D bond energy is about 0.94 ± 0.13 eV stronger than the $Ni_2^+-CD_3$ bond energy. One possible explanation is that the D atom binds at a bridging site whereas CD_3 binds in an atop position, a structural difference that can be rationalized by the directionality of the sp^3 orbital on CD_3 used to form the bond versus the spherical $1s$ orbital on D. For other cluster sizes, it is anticipated that the hydride and methyl bond energies would again be similar to one another. Ni_n^+-CD and Ni_n^+-C bond energies are higher than the Ni_n^+-D values by 3.19 ± 0.23 and 4.00 ± 0.16 eV, respectively, for $n\geqslant3$. The $Ni_n^+-CD_2$ bond energies (lower limits) lie an average of 1.46 ± 0.20 eV higher in energy than the Ni_n^+-D values for $n=3$, 4, 10–16. The $Ni_n^+-CD_2$, Ni_n^+-CD, and Ni_n^+-C bond energies are an average of 1.6 ±0.2, 2.4 ± 0.1, and 2.7 ± 0.2 times stronger, respectively, than the Ni_n^+-D bond energies for $n\geqslant3$. These ratios agree with those for the ratios of H_3C-CH_3 to $H_2C{=}CH_2$ and $HC{\equiv}CH$ and M^+-CH_3 to $M^+{=}CH_2$ and $M^+{\equiv}CH$ bond energies, 1.7 and 2.5, respectively.[76] These observations are qualitatively consistent with formation of single (D and CD_3) vs double (CD_2) vs triple (CD and C) bonds, as anticipated from the bonding character of the ligands.

In our previous work,[17] the patterns in the Ni_n^+-D bond energies as a function of cluster size were used to qualitatively probe the cluster geometry and electronic configuration. Compared to the metal-metal Ni_n^+-Ni bonds, the nickel-deuteride bonds are generally weaker, with a difference of about 0.5 eV that can be attributed to metal-metal bonds enhanced by $3d$-$3d$ interactions. However, $D(Ni_{12}^+-Ni)$ is much stronger (0.9 eV) than $D(Ni_{12}^+-D)$ and $D(Ni_{13}^+-Ni)$ is comparable to $D(Ni_{13}^+-D)$, which is believed to indicate that Ni_{13}^+ clusters have particularly stable geometries. Consequently, substitution of a nickel atom in Ni_{13}^+ by D destroys the symmetry of the cluster, thereby affecting its stability.

Discussion of the bonding of CD_2 to nickel clusters is speculative as nothing is known about the structures of these cluster species. As noted above, the bond energies of CD_2 to Ni_n^+ clusters indicate that two bonds are formed. Presumably, CD_2 could bind terminally to the cluster by forming a σ and a π bond with a single metal atom or could bridge across two metal centers by forming two σ bonds. Ni^+ ($^2D,3d^9$) must bind to CD_2 terminally and has a bond energy weakened by the need to spin decouple two $3d$ electrons from the other nonbonding $3d$ electrons. This promotion energy lowers the Ni^+-CD_2 bond energy (3.17 ± 0.04 eV) from an intrinsic metal-carbon double bond energy of about 4.3 ± 0.1 eV.[76,82] For larger clusters ($n=3,4,10-16$), the $Ni_n^+-CD_2$ bonds are stronger than Ni_n^+-D bonds by 1.5 ± 0.2 eV, which is a little smaller than the intrinsic metal-carbon π bond (1.8 eV).[76] Either there are barriers of about 0.3 ± 0.2 eV to the formation of $Ni_n^+-CD_2$ in reactions (4), as discussed further below, or these nickel clusters require additional promotion to form the π bond beyond the promotion energy needed to form the σ bond.

Bonds between CD and C ligands and the Ni^+ monomer are much weaker than those for larger clusters, and are discussed elsewhere.[60] The bond energies of $Ni_2^+-CD_2$, Ni_2^+-CD, and Ni_2^+-C are quite similar, suggesting that the nickel dimer cation can form two covalent bonds, but not a third. The CD and C ligands can potentially bind to clusters in different ways: terminal, twofold bridging, and threefold bridging. An obvious implication of the strength of the CD and C bonds relative to CD_2 bonds for the trimer and larger clusters is that binding to three atoms in a threefold site may provide the strongest bond energies, consistent with the known structure of alkylidynes bound to many surfaces.[83] Theoretical studies of these small molecules would be of interest in further understanding these trends. For $n\geqslant3$, $D(Ni_n^+-CD)$ values do increase somewhat as the cluster size increases, such that the average BDE is 5.15 ± 0.14 eV for $n=3-9$ and 5.91 ± 0.16 eV for $n=10-16$. For C binding to nickel clusters, $D(Ni_5^+-C)>D(Ni_4^+-C)>D(Ni_3^+-C)$, but for $n\geqslant5$, $D(Ni_n^+-C)$ are nearly constant with an average bond energy of 6.44 ± 0.15 eV. Overall, the Ni_n^+-C bond energies are stronger than $D(Ni_n^+-CD)$ by an average of 1.01 ± 0.35 eV for $n=3-9$ and by 0.62 ± 0.10 eV for $n=10-16$, where they parallel one another quite closely. This difference may be explained by the following argument. The ^3P ground state of the carbon atom can make three bonds (two covalent bonds and a dative bond formed by accepting electron density into the empty $2p$ orbital). In contrast, CD makes three covalent bonds using its $\tilde{a}\,^4\Sigma^-$ state, which lies 0.72 eV above its $X\,^2\Pi_r$ ground state,[81] thereby lowering the final bond energy to nickel clusters. This suggests that nickel clusters have substantial flexibility in making the strongest possible bond to molecular fragments.

B. Bond energies compared to analogous iron clusters

It is useful to compare the binding of D and CD_x species to nickel cluster cations with that to iron cluster cations.[15] For small clusters, the bond energies for D and CD_x to Ni_n^+ and Fe_n^+ vary considerably with cluster size, indicating changes in the electronic structure of the metal clusters.[15] For the dimers, D, CD_3, CD_2, CD, and C bind to Ni_2^+ more strongly than to Fe_2^+ by 1.59, 0.21, 1.01, 1.79, and 0.60 eV, respectively. Clearly, the details of the electronic structure for the dimer species are controlling features in these various bonds, which can be explained by using promotion energy arguments, as previously discussed for D atom bonding to iron cluster cations.[8] The Ni_2^+ dimer has a configuration of $(4s\sigma_g)^2d_A^9d_B^8$,[55] which is formed by combining $Ni^+(^2D,3d^9)$ with $Ni(^3F,4s^23d^8)$. Fe_2^+ is formed by the combination of ground state $Fe(4s^23d^6)$ and ground state $Fe^+(3d^7)$ and believed to have a $(4s\sigma_g)^2d_A^6d_B^7$ electronic configuration.[8] A plausible explanation for the differences in bond energies between Ni_2^+ and Fe_2^+ is simply that spin decoupling the electrons needed for bonding costs more energy in the iron case because of the larger number of unpaired spins involved. Clearly, *ab initio* calculations on such species would be very useful in understanding the details of these bond energies, but are beyond the scope of this experimental study. For $n=3$ and 4, iron and nickel clusters bond energies to CD_x species are very similar, except that the $Ni_3^+-CD_2$ bond is 0.90 eV stronger than $Fe_3^+-CD_2$. Overall, this indicates that the effect of the electronic structure on binding D and CD_x species becomes smaller as the clusters get larger.

Both $D_0(Ni_n^+-CD_x)$ and $D_0(Fe_n^+-CD_x)$ rapidly reach plateaus with increasing cluster size. For larger clusters, $n \geqslant 10$, the bond energies for Ni_n^+ to D, C, CD, and CD_2 (2.6 ± 0.1, 6.5 ± 0.1, 5.9 ± 0.2 and $\geqslant 3.9\pm0.1$ eV) are similar to the values of $D_0(Fe_n^+-D)$, $D_0(Fe_n^+-C)$, $D_0(Fe_n^+-CD)$, and $D_0(Fe_n^+-CD_2)$ (2.6 ± 0.1, 6.1 ± 0.4, 5.9 ± 0.4, and 4.2 ± 0.4 eV, respectively). Clearly, D, C, CD, and CD_2 binding to nickel and iron metal clusters have the same bond orders (single, triple, triple, and double bonds, respectively). The carbide bond energies to nickel are slightly stronger than those to iron, by about 0.4 eV, which may simply be because Ni has more electrons than Fe, which allows better donation to the empty *p* orbital on a C atom. Given the good correspondence between the nickel and iron cluster bond energies, we might expect that Ni_n^+ bonds to CD_2 should be at least the same or perhaps a little stronger than Fe_n^+ bonds to CD_2 for $n \geqslant 10$. Instead, the $Fe_n^+-CD_2$ bond energies are about 0.3 ± 0.4 eV stronger than those for $Ni_n^+-CD_2$. This is another indication that the $Ni_n^+-CD_2$ bond energies from reaction (4) seem to be a little lower than the thermodynamic values, which indicate small barriers to this reaction that are on the order of 0.3 ± 0.4 eV.

C. Bond energies compared to bulk phase values

One area where cluster studies may provide insight into condensed phase chemistry lies in the determination of thermochemistry for species bound to surfaces, especially molecular fragments. We have recently noted that bond energies of oxygen to nickel clusters $n \geqslant 5$ are relatively constant at about 4.6 ± 0.2 eV (Ref. 19) and match bulk phase desorption enthalpies of oxygen to nickel 111 surfaces, 4.6 eV, as measured by calorimetry experiments.[84,85] Likewise, Ni_n^+-D bond energies[17] reach a relatively constant value (Fig. 6) of 2.6 ± 0.1 eV for $n \geqslant 10$. This is close to the bulk phase value for hydrogen binding to bulk nickel surfaces, about 2.7 eV for measurements on Ni(100), Ni(110), and Ni(111) surfaces, Fig. 6.[86]

For carbon based species, the binding of C to nickel surfaces has been measured as about 7.37 eV in a molecular beam experiment,[87] but Siegbahn and Wahlgren[88] note that "this value is suspiciously close to the sublimation energy of graphite" of 7.42 eV and "might therefore have been overestimated." A value for carbon on nickel surfaces obtained using a small Ni_5 cluster model was estimated as 6.50 eV using the bond order conservation (BOC) approach[88] and another value of 6.35 eV for carbon on Ni(111) at a fcc site is obtained using a plane wave slab approach in conjunction with DFT.[46] Calculated values for carbon bound to Ni_7 cluster models are estimated as 4.77 eV at the top site and 7.65 eV at the hollow site using the Amsterdam Density Functional computer program.[48] These various theoretical estimates for surface nickel-carbides span values comparable to our Ni_n^+-C bond energies, which are an average of about 6.5 ± 0.1 eV for larger clusters ($n \geqslant 10$).

In contrast to the atomic H, O, and C systems, there is no experimental information on the thermochemistry of molecular fragments (CH, CH_2, and CH_3) bound to metal surfaces, although such information has been estimated.[43,50,89,90] The successful comparison of surface chemisorption energies for H and O atoms to the bond energies for larger cluster ions suggests that our cluster thermochemistry can be used to estimate surface binding energies for molecular fragments, which are largely inaccessible to experimental measurement. This was also argued in our analogous work for CD_x and ND_x ($x=0-2$) fragments binding to iron cluster cations.[15,20] Our recommended values, taken from the average values for clusters larger than ten atoms, are $D(Ni_n^+-CD)=5.9 \pm 0.2$ eV, $D(Ni_n^+-CD_2) \geqslant 3.9\pm0.1$ eV, and $D(Ni_n^+-CD_3) = 2.6\pm0.1$ eV [assumed to equal the $D(Ni_n^+-D)$ values, however, see discussion below].

Our experimental estimates can be compared to theoretical values for surface binding energies. The bond energies of CH, CH_2, and CH_3 to Ni(111) surfaces have been estimated using many-electron embedding theory as 3.1, 2.9, and 1.8 eV, respectively;[89] using the BOC approach as 5.0, 3.6, and 2.1 eV, respectively;[88,90] and using an *ab initio* cluster model approach as 5.2, 3.8, and 2.1 eV, respectively.[88] The latter two estimated sets are in very good agreement with one another, whereas neither agrees with the embedding estimates. The results of Siegbahn and Wahlgren are expected to be most accurate because these studies utilized bond-prepared clusters, a much larger basis set, and a more thorough correlation treatment.[88] Results of spin-polarized DFT calculations estimated the binding energies for CH_3 on Ni(111) surface as 1.48, 1.46, 1.37, and 1.22 eV at the hcp, fcc, bridge, and top sites, respectively.[50] This DFT study also obtained binding energies for CH_2 at these same sites as 3.22, 3.26, 3.14, and 2.36 eV, respectively. Both sets of values are values well below the estimates above, whereas other DFT calculations[43] found values for CH_2 adsorption energies of 3.73, 2.75, and 2.92 eV at the hollow, bridge, and top sites, respectively. These latter values span the same range as the embedding theory and BOC estimates above. Overall, all of these theoretical estimates provide values below our experimental cluster bond energies for these molecular fragments.

Previously, Siegbahn and Wahlgren pointed out that their calculated chemisorption energies for H to Ni(111) at the threefold hollow site are about 0.2–0.3 eV lower than the experimental surface value (2.7 eV).[88] According to the authors, the chemisorption energy for CH_3 at this site should also be underestimated by a similar amount, such that their best estimated value for CH_3 chemisorption to Ni(111) becomes 2.1–2.4 eV.[88] This is in reasonable agreement with our value for larger clusters $n \geqslant 10$, 2.6 ± 0.1 (using D as a direct analogue for CD_3). However, these calculations also find that nickel clusters bind H atoms more strongly than CH_3 by 0.2–0.5 eV. This may suggest that a better experimental estimate for $D(Ni_n^+-CD_3)$ is $D(Ni_n^+-D)-0.3$ eV $=2.2\pm0.3$ eV, in good agreement with the 2.1–2.4 eV revised estimates from the cluster calculations.

If the calculated chemisorption energies of CH and CH_2 are similarly underestimated, then it may be appropriate to revise the theoretical estimates there as well. We estimate that about 0.6±0.1 and 0.4±0.1 eV should be added to the *ab initio* cluster estimates of 5.2 and 3.8 eV, respectively.[88] (These correction values are 0.2–0.3 eV times 2.5 and 1.7, respectively, the ratio of the cluster-carbon triple and double bonds to single bonds, see above.) Thus, the revised estimates for the chemisorption energies for CH and CH_2 on Ni(111) are about 5.8±0.1 and 4.2±0.1 eV, respectively, in good agreement with our values of 5.9±0.2 eV and $\geqslant$3.9 ±0.1 eV for $n \geqslant 10$, respectively. Overall, these agreements indicate that our bond energies for atomic (H and C) and molecular (CH, CH_2, and CH_3) species bound to larger clusters are reasonable experimental estimates of the binding energies on surfaces.

D. Reaction mechanism

To understand the mechanism of the reactions of nickel cluster cations with methane, we reexamine what is known about the reactions of atomic metal ions with CD_4,[59,60] because the basic principles involved should be the same and proved useful in our $Fe_n^+ + CD_4$ study.[15] For atomic Ni^+, this reaction occurs by C–D bond activation to form a $D-Ni^+-CD_3$ intermediate, which can decompose by simple bond cleavage to form $NiD^+ + CD_3$ or $NiCD_3^+ + D$. The least endothermic process is dehydrogenation, which involves rearrangement of the $D-Ni^+-CD_3$ intermediate to a four-centered transition state involving an incipient D–D bond. The energy of this transition state has been measured to lie 0.58±0.10 eV above the $NiCD_2^+ + D_2$ product asymptote.[60] Because the NiD^+, $NiCD_2^+$, and $NiCD_3^+$ products share the common $D-Ni^+-CD_3$ intermediate, they compete directly with one another. The hydride channel dominates at higher energies because simple cleavage of the Ni–C bond is kinetically more facile than rearrangement over the tight four-centered transition state needed for dehydrogenation. Formation of NiD^+ is favored over $NiCD_3^+$ production because of conservation of angular momentum effects.[91]

The electronic requirements for σ bond activation of CD_4 at a transition metal center can be viewed fairly simply. In order to break the C–D covalent bond and simultaneously form two new bonds between the metal and the D and CD_3 fragments, the metal center must accept electron density from the C–D bond and donate electron density into the antibonding orbital of this bond. Formally, this is an oxidative addition process in which the metal oxidation state increases by 2, although neither the D or CD_3 ligand carries a full negative charge. For atomic first row transition metal ions, the acceptor orbital is largely the $4s$ orbital, and the donor is a $3d\pi$. Combining these orbitals with the bonding and antibonding σ orbitals of the C–D bond leads to pairs of bonding and antibonding molecular orbitals (MOs) for the $D-Ni^+-CD_3$ intermediate. To create the most favorable bonding situation, four electrons are needed to occupy the bonding MOs with no additional electrons for the antibonding MOs. As the C–D bond provides two electrons, the most efficient reaction is expected when the metal has an empty σ acceptor and a doubly occupied π donor.

In analogy with the mechanism for reaction of the monomer with methane, the first step in the reaction of the nickel cluster cations with CD_4 is C–D bond activation to form a $D-Ni_n^+-CD_3$ intermediate. From this intermediate, the major ionic product at higher energies, Ni_nD^+, can be formed by cleaving the Ni–C bond to eliminate an intact methyl group. Once this product is formed, the cross sections for products formed at lower energies ($Ni_nCD_2^+$ and Ni_nC^+) begin to decline, Figs. 1–5, indicating competition between these channels. This competition is also indicated by the fact that accurate Ni_nD^+ bond energies are obtained from the observed thresholds only when competition with dehydrogenation is explicitly considered. The observation of this competition is consistent with all reaction channels sharing the putative $D-Ni_n^+-CD_3$ species as a common intermediate.

For $n=1$, the dehydrogenation reaction (4) is known to occur by a four-centered transition state lying in the exit channel 0.58 eV above the energy of the products.[60] For the dimer reaction, dehydrogenation is also found to have a barrier, which lies 0.61±0.16 eV above the $Ni_2CD_2^+ + D_2$ products. This barrier could again correspond to a four-centered elimination from an intermediate in which both ligands are attached to the same nickel atom. However, another possibility is that the reaction occurs by a five-centered elimination from a $DNi-NiCD_3^+$ intermediate. Such an intermediate is undoubtedly formed as shown by the observation of reaction (10), which forms $NiCD_3^+ + NiD$. Complicating factors in thinking about the likely pathway is whether any of the ligands, D, CD_2, or CD_3, are bridging rather than terminal. Without other information, no definitive conclusions regarding the mechanism of the dehydrogenation process by the nickel dimer cation can be made.

For the dehydrogenation reactions (4) of the larger cluster cations, $n \geqslant 3$, there appear to be small barriers (0.3±0.4 eV) in excess of the endothermicities. In analogy with the mechanism for dehydrogenation reactions of methane by Fe_n^+, it seems likely that these barriers lie in the entrance channel, i.e., in the C–D activation step, rather than in the exit channel. The thresholds measured for $Ni_nCD_2^+$ ($n=3,4,10-16$) formation do not vary appreciably (average of 0.92±0.13 eV, Tables S3–S16). This value is very close to the methane activation energies on various nickel surfaces measured experimentally: 0.73–0.93 eV on Ni(100),[29] 0.77 eV on Ni(111),[30] and 0.90 eV on Ni(111);[47] as well as calculated theoretically: 0.74,[39,40] 1.05,[47] and 1.04 (Ref. 45) eV on Ni(111), and 0.85 eV on Ni(211).[47] The similarity of these values suggests that the thresholds measured here are consistent with barriers for C–D activation energies in the entrance channel, rather than the thermodynamic limits for $Ni_nCD_2^+$ formation. Hence bond energies derived from these thresholds are lower limits to the true thermochemistry for $Ni_nCD_2^+$. We conclude that there are small barriers in excess of the endothermicities for the dehydrogenation reaction (4) of larger clusters, estimated as 0.3±0.4 eV above.

Reactions of larger clusters presumably have the same complicated mechanistic possibilities mentioned for Ni_2^+, i.e., they likely involve $DNi-Ni_{n-1}CD_3^+$ intermediates. In addition, $(NiD)(NiD)(Ni_{n-2}CD_2)^+$ intermediates formed by the migration of two D atoms from the methane to separate nickel atoms, and bridging ligands could be involved. This kind of intermediate is clearly not possible for smaller clusters. Thus, dehydrogenation can occur remotely from the $Ni_n^+-CD_2$ bond, as also suggested in the iron system,[15] which can explain why the barrier in the exit channel observed for $n=1$ and 2 might no longer be rate limiting for larger clusters.

In general, the dehydrogenation reactions (2) and (4) to form Ni_nC^+ and $Ni_nCD_2^+$ products become much more facile with the clusters size increasing. This is clear from the increasing magnitude of the Ni_nC^+ cross sections with cluster size and the fact that the double dehydrogenation reaction *must* occur via a $Ni_nCD_2^+$ transient intermediate. For $n=5-9$, $Ni_nCD_2^+$ products are not observed, presumably because the $Ni_nCD_2^+$ species decompose rapidly to Ni_nC^+ within our experimental time window ($\approx 10^{-4}$ s). However, the lifetimes of reaction intermediates should become longer as the size of the cluster increases, thus allowing the dehydrogenation product, $Ni_nCD_2^+$, to be observed starting at $n=10$. Consistent with this picture is the observation that the maximum magnitude of this cross section gradually increases as the cluster size increases. Even so, the double dehydrogenation reactions to form Ni_nC^+ are still facile in these systems, such that these cross sections are much larger than those of $Ni_nCD_2^+$. The facility of double dehydrogenation is also observed in the $Fe_n^+ + CD_4$ reaction system, although here the single dehydrogenation reaction is observed for all cluster sizes. The facility of dehydrogenation by these metals may be one reason why nickel and iron are used as catalysts industrially in the steam-reforming process, $CH_4 + H_2O \rightarrow CO + 3H_2$.

The formation of $Ni_2CD_3^+$ and Ni_2D^+ in the dimer system must occur by simple bond cleavage from the $D-Ni_2^+-CD_3$ intermediate, similar to the mechanism for reaction of the monomer with methane.[60] Unlike the monomer and dimer, larger nickel clusters do not form $Ni_nCD_3^+$ products. This is likely to be a matter of experimental sensitivity combined with the fact that formation of this product is inhibited by angular momentum conservation considerations. Simply, the reduced mass of the $Ni_nCD_3^+ + D$ product channel is about 2 amu, whereas that for the $Ni_nD^+ + CD_3$ product channel approaches 18 amu, comparable to the reduced mass of the $Ni_n^+ + CD_4$ reactants (about 20 amu). Because orbital angular momentum is largely conserved in these bimolecular reactions, the phase space available to the $Ni_nCD_3^+ + D$ product channel is much smaller than that associated with the $Ni_nD^+ + CD_3$ product channel.

As shown above by thermodynamic arguments, small amounts of $NiCD_3^+ + NiD$ and $Ni_2CD_3^+ + NiD$ are observed for reactions of the dimer and trimer, respectively. The formation of secondary products $Ni_{n-1}CD^+$ is also concomitant with neutral NiD. Clusters larger than Ni_7^+ show an additional path to the formation of $Ni_{n-1}D^+$ corresponding to loss of $NiCD_3$ neutral. These observations provide direct evidence that C–D bond activation by metal clusters produces an intermediate where the D and CD_3 ligands are bound to different nickel atoms, as suggested above. It seems likely that this is true for all clusters even though comparable observations are not made for $n=4-6$. $Ni_{n-1}CD_3^+ + NiD$ products are not observed for larger clusters, $n>3$, probably because this minor channel does not compete effectively with the other major reactions. Failure to observe $NiCD_3$ loss for smaller clusters, $n<7$, may be because smaller clusters have short lifetimes such that there is insufficient time for the migration of D and CD_3 to the remote sites needed for this process.

VI. CONCLUSION

The kinetic energy dependences of the reactions of size-specific nickel cluster cations ($n=2-16$) with deuterated methane are examined in a guided ion beam tandem mass spectrometer. We report cross sections for seven to ten reactions for each cluster system, all of which exhibit thresholds. The main reactions observed are (1), (2), and (4) to form Ni_nD^+, Ni_nC^+, and $Ni_nCD_2^+$, respectively. Analyses of the energy dependence of both primary and secondary routes to Ni_nD^+, Ni_nC^+, and Ni_nCD^+ products provide two independent values for the bond energies for each cluster to D, C, and CD, which are in good agreement. In the case of $Ni_nCD_2^+$, there are barriers of about 0.6 eV in excess of the endothermicity of the initial dehydrogenation reaction for $n=1$ and 2. These barriers are believed to lie in the exit channel.[60] For larger clusters, methane activation to form $Ni_nCD_2^+$ exhibits thresholds of 0.9 ± 0.1 eV values, which are believed to include small barriers (0.3 ± 0.4 eV) in excess of the thermochemistry for dehydrogenation. In analogy with the mechanism for reaction of iron cluster cations with methane,[15] these barriers are believed to lie in the initial dissociative chemisorption steps.

Best estimates for C, CD, CD_2, and CD_3 binding energies to cationic nickel clusters are obtained from analyses of these multiple reactions pathways. The relative magnitudes in D, C, CD, CD_2, and CD_3 bond energies to the nickel cluster cations are consistent with simple bond order considerations (single, triple, triple, double, and single bond orders, respectively). Comparison of these values to limited experimental information for binding of D, C, and O (Ref. 19) atoms to surfaces suggests that our experimental bond energies for larger clusters provide reasonable estimates for heats of adsorption to nickel surfaces. As no experimental information is available for molecular species binding to surfaces, the thermochemistry derived here for clusters bound to CD, CD_2, and CD_3 (using D as a model) provides the first experimental thermodynamic information on such molecular species. These values are in reasonable accord with theoretical estimates for C, CD, CD_2, and CD_3 binding to Ni surfaces.[88]

ACKNOWLEDGMENT

This work was supported by the Chemical Sciences, Geosciences, and Biosciences Division, Office of Basic Energy Sciences, Office of Science, U.S. Department of Energy.

[1] G. W. Parshall, *Homogeneous Catalysis* (Wiley-Interscience, New York, 1980).

[2] B. C. Gates, J. Guczi, and H. Knözinger, *Metal Clusters in Catalysis* (Elsevier, New York, 1986).

[3] P. B. Armentrout, J. B. Griffin, and J. Conceição, in *Progress in Physics of*

Clusters, edited by G. N. Chuev, V. D. Lakhno, and A. P. Nefedov (World Scientific, Singapore, 1999), p. 198.
[4] P. B. Armentrout, Annu. Rev. Phys. Chem. **52**, 423 (2001).
[5] P. B. Armentrout, Eur. J. Mass. Spectrom. **9**, 531 (2003).
[6] M. P. Irion, Int. J. Mass Spectrom. Ion Processes **121**, 1 (1992).
[7] M. B. Knickelbein, Annu. Rev. Phys. Chem. **50**, 79 (1999).
[8] J. Conceição, S. K. Loh, L. Lian, and P. B. Armentrout, J. Chem. Phys. **104**, 3976 (1996).
[9] J. B. Griffin and P. B. Armentrout, J. Chem. Phys. **106**, 4448 (1997).
[10] J. B. Griffin and P. B. Armentrout, J. Chem. Phys. **107**, 5345 (1997).
[11] J. B. Griffin and P. B. Armentrout, J. Chem. Phys. **108**, 8062 (1998).
[12] J. B. Griffin and P. B. Armentrout, J. Chem. Phys. **108**, 8075 (1998).
[13] J. Xu, M. T. Rodgers, J. B. Griffin, and P. B. Armentrout, J. Chem. Phys. **108**, 9339 (1998).
[14] J. Conceição, R. Liyanage, and P. B. Armentrout, Chem. Phys. **262**, 115 (2000).
[15] R. Liyanage, X.-G. Zhang, and P. B. Armentrout, J. Chem. Phys. **115**, 9747 (2001).
[16] R. Liyanage, J. Conceição, and P. B. Armentrout, J. Chem. Phys. **116**, 936 (2002).
[17] F. Liu, R. Liyanage, and P. B. Armentrout, J. Chem. Phys. **117**, 132 (2002).
[18] K. Koszinowski, D. Schröder, H. Schwarz, R. Liyanage, and P. B. Armentrout, J. Chem. Phys. **117**, 10039 (2002).
[19] D. Vardhan, R. Liyanage, and P. B. Armentrout, J. Chem. Phys. **119**, 4166 (2003).
[20] R. Liyanage, J. B. Griffin, and P. B. Armentrout, J. Chem. Phys. **119**, 8979 (2003).
[21] F. Boszo, G. Ertl, M. Grunze, and M. Weiss, Appl. Surf. Sci. **1**, 103 (1977); F. Bsozo, G. Ertl, and M. Weiss, J. Catal. **50**, 519 (1977).
[22] J. B. Benziger, in *Metal-Surface Reaction Energetics*, edited by E. Shustorovich (VCH, New York, 1991), p. 53.
[23] J. R. Rostrup-Nielsen, in *Catalysis: Science and Technology*, edited by J. R. Anderson and M. Boudart (Springer, Berlin, 1984), Vol. 5.
[24] T. P. Beebe, D. W. Goodman, B. D. Kay, and J. T. Yates, J. Chem. Phys. **87**, 2305 (1987).
[25] I. Choekendorff, I. Alstrup, and S. Ullmann, Surf. Sci. **227**, 291 (1990).
[26] B. Ø. Nielsen, A. C. Luntz, P. M. Holmblad, and I. Choekendorff, Catal. Lett. **32**, 15 (1995).
[27] P. M. Holmblad, J. Wambach, and I. Choekendorff, J. Chem. Phys. **102**, 8255 (1995).
[28] J. R. Rostrup-Nielsen, J. Sehested, and J. K. Nørskov, Adv. Catal. **47**, 65 (2002).
[29] P. M. Holmblad, J. H. Larsen, and I. Choekendorff, J. Chem. Phys. **104**, 7289 (1996); J. H. Larsen and I. Choekendorff, Surf. Sci. Rep. **35**, 163 (1999).
[30] R. C. Egebjerg, S. Ullmann, I. Alstrup, C. B. Mullins, and I. Choekendorff, Surf. Sci. **497**, 183 (2002).
[31] A. C. Luntz, J. Chem. Phys. **102**, 8264 (1995).
[32] M.-N. Carre and B. Jackson, J. Chem. Phys. **108**, 3722 (1998).
[33] Y. Xiang, J. Z. H. Zhang, and D. Y. Wang, J. Chem. Phys. **117**, 7698 (2002); **118**, 8954 (2003).
[34] M. B. Lee, Q. Y. Yang, S. L. Tang, and S. T. Ceyer, J. Chem. Phys. **85**, 1693 (1986).
[35] Q. Y. Yang, K. J. Maynard, A. D. Johnson, and S. T. Ceyer, J. Chem. Phys. **102**, 7734 (1995).
[36] M. P. Kaminsky, N. Winograd, G. L. Geoffrey, and M. A. Vannice, J. Am. Chem. Soc. **108**, 1315 (1986).
[37] M. R. A. Blomberg, U. Brandemark, and P. E. M. Siegbahn, J. Am. Chem. Soc. **105**, 5557 (1983).
[38] A. B. Anderson and J. J. Maloney, J. Phys. Chem. **92**, 809 (1988).
[39] H. Yang and J. L. Whitten, J. Chem. Phys. **96**, 5529 (1992).
[40] H. Yang and J. L. Whitten, J. Am. Chem. Soc. **113**, 6442 (1991).
[41] J. Schule, P. Siegbahn, and U. Wahlgren, J. Chem. Phys. **89**, 6982 (1988).
[42] O. Swang, J. K. Faegri, O. Gropen, U. Wahlgren, and P. Siegbahn, Chem. Phys. **156**, 379 (1991).
[43] H. Burghgraef, A. P. J. Jansen, and R. A. van Santen, J. Chem. Phys. **98**, 8810 (1993); **101**, 11012 (1994); Faraday Discuss. Chem. Soc. **96**, 337 (1993); Chem. Phys. **117**, 407 (1993); Surf. Sci. **324**, 345 (1995).
[44] A. P. J. Jansen and H. Burghgraef, Surf. Sci. **344**, 149 (1995).
[45] P. Kratzer, B. Hammer, and J. K. Nørskov, J. Chem. Phys. **105**, 5595 (1996).
[46] R. M. Watwe, H. S. Bengaard, J. R. Rostrup-Nielsen, J. A. Dumesic, and J. K. Nørskov, J. Catal. **189**, 16 (2000).
[47] H. S. Bengaard, J. K. Nørskov, J. Sehested, B. S. Clausen, L. P. Nielsen, A. M. Molenbroek, and J. R. Rostrup-Nielsen, J. Catal. **209**, 365 (2002).
[48] C.-T. Au, M.-S. Liao, and C.-F. Ng, J. Phys. Chem. A **102**, 3959 (1998).
[49] C.-T. Au, C.-F. Ng, and M.-S. Liao, J. Catal. **185**, 12 (1999).
[50] A. Michaelides and P. Hu, J. Chem. Phys. **112**, 6006 (2000); **112**, 8120 (2000); Surf. Sci. **437**, 362 (1999).
[51] S. K. Loh, D. A. Hales, L. Lian, and P. B. Armentrout, J. Chem. Phys. **90**, 5466 (1989).
[52] T. G. Deitz, M. A. Duncan, D. E. Powers, and R. E. Smalley, J. Chem. Phys. **74**, 6511 (1981).
[53] C.-X. Su and P. B. Armentrout, J. Chem. Phys. **99**, 6506 (1993).
[54] D. A. Hales, C.-X. Su, L. Lian, and P. B. Armentrout, J. Chem. Phys. **100**, 1049 (1994).
[55] L. Lian, C.-X. Su, and P. B. Armentrout, J. Chem. Phys. **96**, 7542 (1992).
[56] E. Teloy and D. Gerlich, Chem. Phys. **4**, 417 (1974); D. Gerlich, Adv. Chem. Phys. **82**, 1 (1992).
[57] N. R. Daly, Rev. Sci. Instrum. **31**, 264 (1959).
[58] K. M. Ervin and P. B. Armentrout, J. Chem. Phys. **83**, 166 (1985).
[59] L. F. Halle, P. B. Armentrout, and J. L. Beauchamp, Organometallics **1**, 963 (1982).
[60] F. Liu, X.-G. Zhang, and P. B. Armentrout, Phys. Chem. Chem. Phys. (submitted).
[61] W. J. Chesnavich and M. T. Bowers, J. Phys. Chem. **83**, 900 (1979).
[62] P. B. Armentrout, in *Advances in Gas Phase Metal Ion Chemistry*, edited by N. G. Adams and L. M. Babcock (JAI, Greenwich, 1992), Vol. 1, p. 83.
[63] P. B. Armentrout, Int. J. Mass. Spectrom. **200**, 219 (2000).
[64] F. Muntean and P. B. Armentrout, J. Chem. Phys. **115**, 1213 (2001).
[65] A. A. Shvartsburg, K. M. Ervin, and J. H. Frederick, J. Chem. Phys. **104**, 8458 (1996).
[66] R. J. Birgenean, J. Cordes, G. Dolling, and A. D. Woods, Phys. Rev. A **136**, 1359 (1964).
[67] G. Simmons and H. Wang, *Single Crystal Elastic Constants and Calculated Aggregate Properties: A Handbook*, 2nd ed. (M.I.T., Cambridge, 1971).
[68] T. Shimanouchi, *Table of Molecular Vibrational Frequencies, Consolidated* (National Bureau of Standards, Washington DC, 1972), Vol. I.
[69] K. M. Ervin, Chem. Rev. **101**, 391 (2001).
[70] P. B. Armentrout, J. Am. Soc. Mass Spectrom. **13**, 419 (2002).
[71] R. G. Gilbert and S. C. Smith, *Theory of Unimolecular and Recombination Reactions* (Blackwell Scientific, Oxford, 1990).
[72] D. G. Truhlar, B. C. Garrett, and S. J. Klippenstein, J. Phys. Chem. **100**, 12771 (1996).
[73] K. A. Holbrook, M. J. Pilling, and S. H. Robertson, *Unimolecular Reactions*, 2nd ed. (Wiley, New York, 1996).
[74] M. T. Rodgers, K. M. Ervin, and P. B. Armentrout, J. Chem. Phys. **106**, 4499 (1997).
[75] See EPAPS Document No. E-JCPSA6-121-001446 for 14 figures, 16 tables, and an explanation of the choices for molecular constants used in the data analysis. A direct link to this document may be found in the online article's HTML reference section. The document may also be reached via the EPAPS homepage (http://www.aip.org/pubservs/epaps.html) or from ftp.aip.org in the directory /epaps/. See the EPAPS homepage for more information.
[76] P. B. Armentrout and B. L. Kickel, in *Organometallic Ion Chemistry*, edited by B. S. Freiser (Kluwer, Dordrecht, 1996), p. 1.
[77] Ni–D and Ni–CD_3 bond energies have been adjusted from Ni–H and Ni–CH_3 bond energies (Ref. 76) by considering the differences in zero point energies.
[78] Thermochemistry for deuterated fragments of CD_4 is compiled in C. L. Haynes, Y.-M. Chen, and P. B. Armentrout, J. Phys. Chem. **100**, 111 (1996).
[79] M. T. Rodgers and P. B. Armentrout, J. Chem. Phys. **109**, 1787 (1998).
[80] E. R. Fisher and P. B. Armentrout, J. Phys. Chem. **94**, 1674 (1990).
[81] H. Huber and G. Herzberg, *Constants of Diatomic Molecules* (Van Nostrand Reinhold, New York, 1979).
[82] P. B. Armentrout, L. S. Sunderlin, and E. R. Fisher, Inorg. Chem. **28**, 4436 (1989).
[83] M. R. Albert and J. T. Yates, Jr., *The Surface Scientist's Guide to Organometallic Chemistry* (American Chemical Society, Washington, DC, 1987).
[84] J. B. Benziger and R. E. Preston, Surf. Sci. **141**, 576 (1984).
[85] W. A. Brown, R. Kose, and D. A. King, Chem. Rev. **98**, 797 (1998).
[86] K. Christmann, O. Schober, G. Ertl, and M. Neuman, J. Chem. Phys. **60**, 4528 (1974); J. Lapujoulade and K. S. Neil, *ibid.* **57**, 34 (1972).

[87] L. T. Isett and J. M. Blakely, Surf. Sci. **47**, 645 (1975).
[88] P. E. M. Siegbahn and U. Wahlgren, in *Metal-Surface Reaction Energetics*, edited by E. Shustorovich (VCH, New York, 1991), p. 1.
[89] H. Yang and J. L. Whitten, Surf. Sci. **255**, 193 (1991).
[90] E. Shustorovich, Adv. Catal. **37**, 101 (1990).
[91] R. H. Shultz, J. L. Elkind, and P. B. Armentrout, J. Am. Chem. Soc. **110**, 411 (1988).
[92] J. L. Elkind and P. B. Armentrout, J. Phys. Chem. **90**, 6576 (1986).